Self-Avoiding Wormlike Chain Confined in a Cylindrical Tube: Scaling Behavior

Jeff Z. Y. Chen*

Department of Physics and Astronomy, University of Waterloo, Waterloo, Ontario N2L 3GI, Canada

(Received 18 January 2018; revised manuscript received 27 April 2018; published 18 July 2018)

Within a confining tube section, the multithreads of a strongly confined, backfolding polymer exert the excluded-volume repulsions on each other and produce physical properties that are very different from those of a confined ideal chain. The conformational properties of a such confined wormlike chain are of fundamental interest and are also practically useful in understanding the DNA confinement problems. Here, the excluded-volume effects are added to the standard wormlike-chain model by a self-consistent field theory. The numerical solutions are examined in light of their scaling properties.

DOI: 10.1103/PhysRevLett.121.037801

Introduction.—The last decade has witnessed dramatic progress in understanding the physical properties of a confined, long semiflexible chain where a number of basic physical length scales compete against each other. The subject matter connects two classical pictures in polymer physics: de Gennes's for a weakly confined flexible polymer and Odijk's for a strongly confined semiflexible chain. As experimental applications (in studying, for example, confined DNA conformations within various environments) [1–13] of theoretical results [14–24] lie somewhere in between the weak and strong confinement limits, the elucidation of the experimental and computer-simulation results [22,25–41] in terms of basic concepts established in polymer physics becomes practically and fundamentally important.

Most real polymer chains, such as DNA molecules, resemble a cylindrical filament that has a nonzero diameter d. The physical properties of a confined, ideal wormlike-chain model (i.e., $d = 0$) [42–44] are now relatively well understood. Consider a wormlike chain of length L confined in a cylindrical tube of diameter D [see Figs. 1(a)–1(d)]. In a standard model, in free space the persistence length P is a basic scale below which the polymer segment cannot easily bend. Two emergent length scales are usually used to describe the tube-confinement problem: the deflection length λ that describes the length of a typical polymer segment that is free from wall contact [45], and the global persistence length g beyond which the polymer makes hairpin turns [17], both as functions of D/P. These length scales are explored through Monte Carlo (MC) simulations [14–16,19,29,38,39] and quantitative solutions to the wormlike-chain model [23,24].

The physical properties of a confined, self-avoiding wormlike-chain model ($d \neq 0$) build on those of an ideal chain and display their own distinct scaling behavior. For a long polymer chain ($L \gg g$, assumed here), it is expected that the reduced physical properties depend on *two* parameters $\tilde{d} = d/P$ and $\tilde{D} = D/P$. Using λ and g, Odijk unraveled new power laws for a self-avoiding chain [20] within the "backfolded Odijk regime" [36] [simply referred to as the "Odijk regime" here, shown in Fig. 1(e)]. Recently, Dorfman's group has claimed that this distinct regime was observed and verified using their MC data for confinement in a square tube [36], circular tube [38], and rectangular tube [39]. This regime is also believed to exist for DNA confinement in a recent review [46]. Using a "telegraph" comparison, Werner *et al.* developed a *one*-parameter theory [41] in an attempt to capture experimental data in a universal view; there are, however, obvious deviations of some data from their theory.

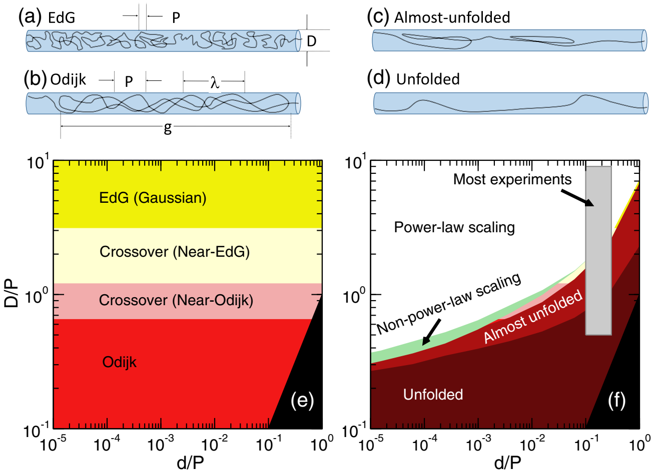

FIG. 1. Length scales in the wormlike-chain confinement problem. Plots (a)–(d) illustrate the physical scales of the extended de Gennes (EdG) regime, Odijk regime, almost unfolded regime, and unfolded regime. Plot (e) quantitatively defines the Odijk regime according to the SCFT solution of the free energy. Plot (f) summarizes main findings of the present work, which identifies the scaling behavior in the white and green areas, in terms of reduced excluded-volume diameter d/P and confinement tube diameter D/P. The recent experimental results on DNA confinement are conducted for systems having parameters in the gray area.

This Letter presents a rigorous solution to the confined self-avoiding wormlike-chain problem with both $\tilde{d}$ and $\tilde{D}$ originally present in a standard model. The study indicates that *unified* scaling laws as powers of a single scaling parameter ξ exist in a large parameter area, covering the extended de Gennes (EdG), crossover, and Odijk regimes [Fig. 1(f)], which agrees with the assessment of Ref. [41]. A non-power-law scaling regime of a single ξ exists only in a very narrow corridor. Beyond these, however, the physical properties depend on both $\tilde{d}$ and ξ. Most recent simulation data [36,38] and certainly the DNA thickness dimensions (summarized in Ref. [41]) either fall *outside* of the Odijk regime or need to be described by a two-parameter theory.

Methods.—The calculation is based on the wormlike-chain model, in which a linear polymer is described by a continuous curve. A contour variable s, within the range $[0, L]$, is specified along the curve, for a chain having a total contour length L. The spatial position of a point on the curve at s is represented by the three-dimensional vector $\mathbf{r}(s)$. The unit vector $\mathbf{u}(s) = d\mathbf{r}/ds$ determines the tangent direction. The probability distribution for a given configuration is assumed to be $\mathcal{P} = \exp(-H_0 - H_{\text{int}})$, where the reduced Hamiltonian

$$H_0 \equiv \frac{P}{2}\int_0^L ds \left(\frac{d\mathbf{u}}{ds}\right)^2 \tag{1}$$

is for a chain without the excluded volume and

$$H_{\text{int}} = d\int_0^L ds \int_0^L ds' \delta[\mathbf{r}(s) - \mathbf{r}(s')]|\mathbf{u}(s) \times \mathbf{u}(s')| \tag{2}$$

is for the excluded volume interaction between the polymer segments at s and s'. The $\mathbf{u}$-dependent vector cross product involves the relative orientations of two polymer segments, which was introduced originally by Onsager [47]. The mathematical difficulty of exactly treating H_{int} is widely known.

In this work the well-developed self-consistent field theory (SCFT) in polymer physics is used, in which H_{int} is replaced by an external potential field W. The connection between W and H_{int} is made through the saddle-point approximation. This enables the analysis and numerical calculation of the Green's function, as the solution to a differential equation. For a long-chain problem $L \gg P$, the "ground-state-dominating" procedure is taken. The technical details can be found elsewhere [48]. The main findings are summarized here.

Scaling properties.—The polymer extension along the axial direction $\langle Z\rangle$ is an experimentally accessible quantity. The reduced extension $\tilde{Z} \equiv \langle Z\rangle/L$ has the asymptotic limits $\tilde{Z} \to 0$ (as $\tilde{d} \to 0$) and $\tilde{Z} \to 1$ (in the fully unfolded state). The calculation of $\tilde{Z}$ can be realized by using an auxiliary field [49] in a SCFT and covers the entire $\tilde{Z}$ range over (0, 1). A special case is small $\tilde{Z}$; an analytical deduction yields a power law,

$$\tilde{Z} = \xi^{1/3}, \tag{3}$$

with the definition

$$\xi \equiv \tilde{d}\chi_0(\tilde{D})C_0(\tilde{D})/\tilde{D}^2, \tag{4}$$

based on a first-order perturbation expansion in $\xi^{1/3}$.

The definition of ξ can be elucidated from a balance between the entropy penalty of stretching a wormlike polymer to a mean length $\langle Z\rangle$ and the mean excluded-volume energy, in terms of a classical Flory argument. The former is similar to that of a Gaussian chain $Z^2/LP\chi_0$, where the denominator is the mean square end-to-end distance of a confined ideal wormlike chain, and the latter is the Onsager excluded volume energy for the volume $\langle Z\rangle\pi D^2/4$ occupied by the polymer, $[(L/2P)^2/\langle Z\rangle D^2]dP^2C_0$ [44]. Minimizing the sum of these with respect to $\langle Z\rangle$ yields the power law above, within a constant prefactor.

Both $\chi_0(\tilde{D})$, which is proportional to g [24,39], and the orientationally dependent excluded-volume energy $C_0(\tilde{D})$ are functions of the cross-section geometry of the confinement. Their full $\tilde{D}$ dependencies for a cylindrical-tube confinement are numerically evaluated here and displayed in Fig. 2. The asymptotic behavior at large $\tilde{D}$ is exact and small $\tilde{D}$ empirical,

$$\chi_0(\tilde{D}) = \begin{cases} 2/3, & \text{when } \tilde{D} \gg 1, \\ 2e^{2E_m/\tilde{D}}/(B_2\tilde{D})^{1/2} & \text{when } \tilde{D} \ll 1, \end{cases} \tag{5}$$

$$C_0(\tilde{D}) = \begin{cases} 2.0984\ldots, & \text{when } \tilde{D} \gg 1, \\ (1.21 \pm 0.01)\tilde{D}^{1/3} & \text{when } \tilde{D} \ll 1, \end{cases} \tag{6}$$

where $E_m = 1.435\,57$ and $B_2 = 5.9560$. These asymptotes are plotted in Fig. 2.

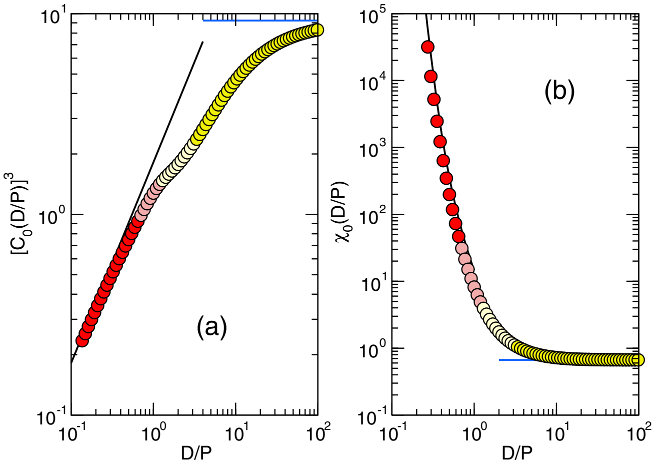

FIG. 2. (a) Cubic $C_0(\tilde{D})$ and (b) $\chi_0(\tilde{D})$ as functions of $\tilde{D}$ for cylindrical-tube geometry. Circles represent the numerical solutions to the SCFT. The two asymptotic limits, shown by black and blue lines, are those in Eqs. (5) and (6). The meanings of symbol colors are the same as in Fig. 1(e).

On one hand, in the $\tilde{D} \gg 1$ limit, Eqs. (3) and (4) reduce to the scaling properties of the EdG regime and on the other hand, in the $\tilde{D} \ll 1$ limit, the Odijk regime [20]. Hence it is a unified version, as long as $\xi \ll 1$. The existence of a scaling parameter ξ was noted by Werner *et al.* in their analysis of a "telegraph scaling theory" where a similar parameter α was identified [41].

Figure 3(a) shows the numerical solutions of SCFT for $\tilde{Z}(\tilde{d}, \tilde{D})$ as a function of $\tilde{D}$ for various values of $\tilde{d}$, when cylindrical confinement is considered. The converted scaling plot for $\tilde{Z} = \zeta(\tilde{d}, \xi)$ is displayed in plot (b). The dependence of $\zeta(\tilde{d}, \xi)$ on $\xi^{1/3}$ is linear when $\xi \ll 1$, as demonstrated by the collapsing of data points in Fig. 3(a) to the single line in 3(b). The separation between EdG and Odijk regimes is artificial—the light yellow and yellow circles (in EdG) and red and pink circles (in Odijk) share the same power-law line, including the crossover. The white area in Fig. 1(f) is where $\tilde{Z}(\tilde{d}, \tilde{D})$ can be represented by $\xi^{1/3}$ within 2% accuracy.

The free energy per unit segment of length $P\chi_0$ is a quantity that can be probed by using advanced Monte Carlo techniques [38,39] and its experimental observations could be made by creative approaches utilizing nonuniform confinement dimensions [52,53]. The saddle-point approximation of SCFT directly yields an expression for the free energy. Within the $\xi \ll 1$ limit, the SCFT yields a free-energy difference $\Delta F(\tilde{d}, \tilde{D}) = F(\tilde{d}, \tilde{D}) - F(0, \tilde{D})$ that follows the unified power law,

$$(P\chi_0/L)\beta\Delta F = (3/2)\xi^{2/3}, \tag{7}$$

where β is the inverse temperature. The same $\xi^{2/3}$ power law can be deduced from a simple Flory argument; here the SCFT exactly pins down the coefficient 3/2 from a perturbation expansion in ξ, regardless of the cross-section geometry of the confinement tube, as long as it has a reasonable shape. The full numerical solution to SCFT for the cylindrical confinement produces a F depending on both $\tilde{d}$ and $\tilde{D}$ as illustrated in Fig. 3(c). The scaling plot in Fig. 3(d), $\Phi(\tilde{d}, \xi) \equiv (P\chi_0/L)\beta\Delta F(\tilde{d}, \tilde{D})$, indeed follows this power law in the small ξ regime.

What happens beyond the small-ξ regime? Originally the physical system itself inherently depends on two parameters $\tilde{d}$ and $\tilde{D}$. Take $\tilde{Z} = \tilde{Z}(\tilde{d}, \tilde{D})$ presented in Fig. 3(a) as an example; instead of the pair $\tilde{d}$ and $\tilde{D}$, the pair $\tilde{d}$ and ξ can be used by realizing that all $\tilde{D}$ dependence is replaceable by the well-defined Eq. (4) above. Then, $\tilde{Z} = \zeta(\tilde{d}, \xi)$ is a two-parameter function. Figure 3(b) shows ζ as functions of ξ for various specified values of $\tilde{d}$.

This two-parameter dependence becomes a single ξ dependence under two circumstances. One is the $\xi \ll 1$ regime already discussed (regardless of the sizes of $\tilde{d}$ and $\tilde{D}$), when the function $\zeta(\tilde{d}, \xi)$ merges to a unified power

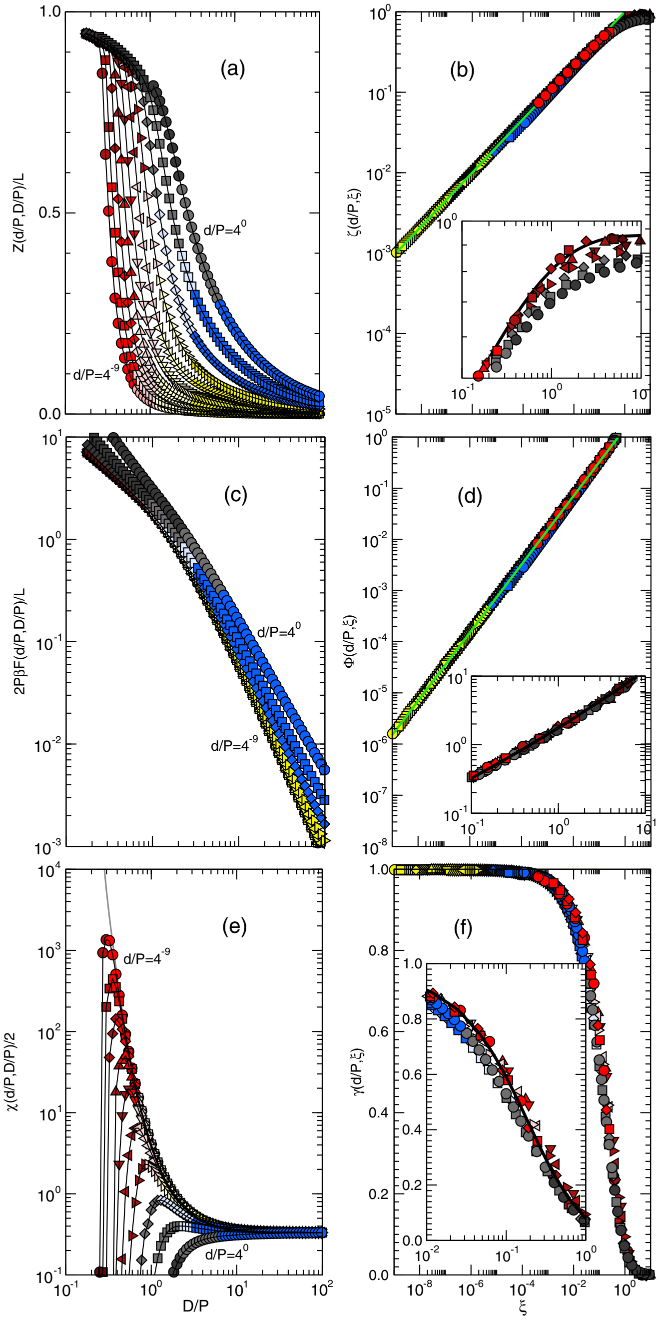

FIG. 3. (a)–(b) Polymer extension Z, (c)–(d) free energy F, and (e)–(f) mean-square extension deviation as functions of $\tilde{d}$ and $\tilde{D}$ (left panels) as well as $\tilde{d}$ and ξ (right panels). The original SCFT solutions are displayed in (a), (c), and (e) where deep-dark red and deep gray circles represent systems in the unfolded state, dark red and gray in the almost-unfolded state, red in the Odijk regime, pink, light yellow, light blue in the crossover region, and yellow and blue in the EdG regime. The 10 curves, from right to left in (a), correspond to $\tilde{d} = 4^0, 4^{-1}, \ldots, 4^{-9}$. The scaled versions in (b), (d), and (f) contain all original data, after ξ is calculated from $[\tilde{d}, \tilde{D}]$ according to Eq. (4) in which χ_0 and C_0 are presented in Fig. 2. The green straight lines in (b) and (d) represent Eqs. (3) and (7). The insets show the nonlinearity where solid black curves represent $\zeta(0, \xi)$, $\Phi(0, \xi)$, and $\gamma(0, \xi)$, for which the empirical expressions can be found in the Supplemental Material [50].

law. The second case is near the Odijk regime when both $\tilde{d} \ll 1$ and $\tilde{D} \leq 1$. Note that for a small $\tilde{d}$, ξ can be any value, adjusted by exponentially large χ_0 of a small-$\tilde{D}$ system. A nonlinear regime in the log-log plot of Fig. 3(b) is entered, where asymptotically a one-parameter, non-power-law function $\zeta(0, \xi)$ exists. The green area in Fig. 1(f) is where $\tilde{Z}(\tilde{d}, \tilde{D})$ can be represented by a non-power law $\zeta(0, \xi)$ within 2% accuracy.

Hence, when $\tilde{d} \gtrsim 10^{-2}$, $\tilde{Z}$ must be described by a two-parameter model beyond the power-law regime, as shown in Fig. 1(f) and the inset of Fig. 3(b). This is evident in Ref. [41], in which a one-parameter theory for cases where hairpins dominate the configuration of the chain and alignment fluctuations can be ignored is compared to the experimental measurements. Signs of the need for a two-parameter model can already be viewed from their Fig. 4(c), as the data for most systems with larger $\tilde{d}$ and $\tilde{D}$ deviates more from their own $\zeta(0, \xi)$ curve.

Finally, the mean-square deviation of the polymer extension from the main value is examined here,

$$\langle (Z - \langle Z \rangle)^2 \rangle \equiv LP\chi(\tilde{d}, \tilde{D}), \qquad (8)$$

in terms of $\chi(\tilde{d}, \tilde{D})$ as plotted in Fig. 3(e). At $\tilde{d} = 0$, $\chi_0 \equiv \chi(0, \tilde{D})$ is shown as the gray curve in the background, which is directly proportional to g defined in Refs. [17,20]; it explodes exponentially in large $1/\tilde{D}$. From extremely small $\tilde{d}$, illustrated here to demonstrate the asymptotic behavior, to a moderate $\tilde{d}$, $\chi(\tilde{d}, \tilde{D})$ follows $\chi(0, \tilde{D})$ until reaching a peak, where $\tilde{Z}$ is approximately 0.5. It is in this parameter regime where the scaled $\gamma(\tilde{d}, \xi) \equiv \chi(\tilde{d}, \tilde{D})/\chi(0, \tilde{D})$ remains 1 universally, shown in Fig. 3(f). It is also the regime where $\tilde{Z}$ and ΔF have power laws.

The fact that the left-hand side of (8) is proportional to LP has been employed when simulation data [39,46] and experimental measurements [41] are analyzed, whereas the fact that it must reduce to $LP\chi(0, \tilde{D})$ (hence $2Lg$) for small ξ is not widely appreciated. Often, a constant ratio $\chi(\tilde{d}, \tilde{D})/g$ is determined from computer simulation data, different from 1. It is not clear whether this is because the original computer simulations were performed for a non-asymptotically small $\tilde{d}$, or the determination of g was off by a numerical factor.

Beyond the peak and before $\chi(\tilde{d}, \tilde{D})$ drastically decreases, the polymer is in an almost unfolded state where $\tilde{Z} \gtrsim 0.5$. Except for a small region [Fig. 1(f), green] where the non-power-law scaling function $\gamma(0, \xi)$ exists, in most cases the SCFT solution of $\gamma(\tilde{d}, \xi)$ deviates from the asymptotic $\gamma(0, \xi)$, as shown by the inset of Fig. 3(f), which is consistent with the analysis of the $\zeta(\tilde{d}, \xi)$ data.

As $\tilde{D}$ decreases further, the polymer reaches an unfold state. The occurrence of the maximum curvature of the $\gamma(\tilde{d}, \xi)$ curve at the low-right corner of Fig. 3(f) is used here as the division between the almost-unfolded and unfolded states, shown in Fig. 1(f). This happens approximately at $\xi \sim 1$. The system now runs into the "classical Odijk regime," termed after Refs. [36,38,39,46], which is a well studied subject [14–16,19,21,23]. The numerical SCFT data for $\tilde{Z}$ and χ, for example, now approaches the known scaling laws [19,21], $\tilde{Z} = 1 - (0.1701\ldots)\tilde{D}^{2/3}$ and $\chi = (0.00754\ldots)\tilde{D}^2$, as functions of $\tilde{D}$, not ξ.

Summary.—According to the numerical solution to the self-consistent field theory for a self-avoiding wormlike polymer chain, the validity of various scaling properties is critically examined for the polymer extension, free energy, and extension variance, in the $[\tilde{d}, \tilde{D}]$ parameter space. A new perspective, which can be used to divide the scaling behavior, is presented as Fig. 1(f). The main results include the prediction and verification of a unified power law regime, the indication of the need for a complete two-parameter theory rather than one-parameter theory, and the clarification of the properties of the extension variance over the entire parameter space.

The present calculation is based on a mean-field approach, unifying the physical picture previously divided into extended de Gennes, backfolding Odijk, classical Odijk (unfolded) regimes, and their crossovers. In the polymer literature, and certainly the DNA confinement literature, there is a concern of whether a distinct de Gennes blob regime exists for a self-avoiding tube-confined polymer, expected at a relatively large $\tilde{D}$ [27,32]. It remains a challenge to incept a blob concept into the self-consistent field theory for the current problem. When it happens, the top if Fig. 1(f) could be augmented by another division line for the de Gennes blob regime.

The original data can be found by following the link in Ref. [50].

Financial support from the Natural Sciences and Engineering Council of Canada is gratefully acknowledged. This work was made possible by the facilities of the Shared Hierarchical Academic Research Computing Network and Compute Canada.

---

[*] jeffchen@uwaterloo.ca

[1] W. Reisner, K. J. Morton, R. Riehn, Y. M. Wang, Z. Yu, M. Rosen, J. C. Sturm, S. Y. Chou, E. Frey, and R. H. Austin, Phys. Rev. Lett. **94**, 196101 (2005).

[2] W. Reisner, J. P. Beech, N. B. Larsen, H. Flyvbjerg, A. Kristensen, and J. O. Tegenfeldt, Phys. Rev. Lett. **99**, 058302 (2007).

[3] L. H. Thamdrup, A. Klukowska, and A. Kristensen, Nanotechnology **19**, 125301 (2008).

[4] C. Zhang, F. Zhang, J. A. van Kan, and J. R. C. van der Maarel, J. Chem. Phys. **128**, 225109 (2008).

[5] J. T. D. Bonis-O'Donnell, W. Reisner, and D. Stein, New J. Phys. **11**, 075032 (2009).

[6] Y. Kim, K. S. Kim, K. L. Kounovsky, R. Chang, G. Y. Jung, J. J. dePablo, K. Jo, and D. C. Schwartz, Lab Chip **11**, 1721 (2011).

[7] W. Reisner, J. N. Pedersen, and R. H. Austin, Rep. Prog. Phys. **75**, 106601 (2012).

[8] D. Gupta, J. Sheats, A. Muralidhar, J. J. Miller, D. E. Huang, S. Mahshid, K. D. Dorfman, and W. Reisner, J. Chem. Phys. **140**, 214901 (2014).

[9] V. Iarko, E. Werner, L. K. Nyberg, V. Müller, J. Fritzsche, T. Ambjörnsson, J. P. Beech, J. O. Tegenfeldt, K. Mehlig, F. Westerlund, and B. Mehlig, Phys. Rev. E **92**, 062701 (2015).

[10] D. Gupta, J. J. Miller, A. Muralidhar, S. Mahshid, W. Reisner, and K. D. Dorfman, ACS Macro Lett. **4**, 759 (2015).

[11] M. Alizadehheidari, E. Werner, C. Noble, M. Reiter-Schad, L. K. Nyberg, J. Fritzsche, B. Mehlig, J. O. Tegenfeldt, T. Ambjörnsson, F. Persson, and F. Westerlund, Macromolecules **48**, 871 (2015).

[12] W. F. Reinhart, J. G. Reifenberger, D. Gupta, A. Muralidhar, J. Sheats, H. Cao, and K. D. Dorfman, J. Chem. Phys. **142**, 064902 (2015).

[13] J.-W. Yeh and K. Szeto, ACS Macro Lett. **5**, 1114 (2016).

[14] M. Dijkstra, D. Frenkel, and H. N. Lekkerkerker, Physica (Amsterdam) **193A**, 374 (1993).

[15] T. W. Burkhardt, J. Phys. A **28**, L629 (1995).

[16] D. J. Bicout and T. W. Burkhardt, J. Phys. A **34**, 5745 (2001).

[17] T. Odijk, J. Chem. Phys. **125**, 204904 (2006).

[18] J. Z. Y. Chen and D. E. Sullivan, Macromolecules **39**, 7769 (2006).

[19] Y. Yang, T. W. Burkhardt, and G. Gompper, Phys. Rev. E **76**, 011804 (2007).

[20] T. Odijk, Phys. Rev. E **77**, 060901 (2008).

[21] T. W. Burkhardt, Y. Yang, and G. Gompper, Phys. Rev. E **82**, 041801 (2010).

[22] L. Dai, S. Y. Ng, P. S. Doyle, and J. R. C. van der Maarel, ACS Macro Lett. **1**, 1046 (2012).

[23] J. Z. Y. Chen, Macromolecules **46**, 9837 (2013).

[24] J. Z. Y. Chen, Phys. Rev. Lett. **118**, 247802 (2017).

[25] Y.-L. Chen, H. Ma, M. D. Graham, and J. J. de Pablo, Macromolecules **40**, 5978 (2007).

[26] P.-K. Lin, K.-H. Lin, C.-C. Fu, K.-C. Lee, P.-K. Wei, W.-W. Pai, P.-H. Tsao, Y.-L. Chen, and W. S. Fann, Macromolecules **42**, 1770 (2009).

[27] Y. Wang, D. R. Tree, and K. D. Dorfman, Macromolecules **44**, 6594 (2011).

[28] P.-K. Lin, C.-C. Hsieh, Y.-L. Chen, and C.-F. Chou, Macromolecules **45**, 2920 (2012).

[29] M. R. Smyda and S. C. Harvey, J. Phys. Chem. B **116**, 10928 (2012).

[30] R. Chang and K. Jo, J. Chem. Phys. **136**, 095101 (2012).

[31] Z. Benkova and P. Cifra, Macromolecules **45**, 2597 (2012).

[32] D. R. Tree, Y. Wang, and K. D. Dorfman, Phys. Rev. Lett. **110**, 208103 (2013).

[33] L. Dai, D. R. Tree, J. R. C. van der Maarel, K. D. Dorfman, and P. S. Doyle, Phys. Rev. Lett. **110**, 168105 (2013).

[34] L. Dai, J. van der Maarel, and P. S. Doyle, Macromolecules **47**, 2445 (2014).

[35] Y. Pollak, S. Goldberg, and R. Amit, Phys. Rev. E **90**, 052602 (2014).

[36] A. Muralidhar, D. R. Tree, and K. D. Dorfman, Macromolecules **47**, 8446 (2014).

[37] T. S. C. Smithe, V. Iarko, A. Muralidhar, E. Werner, K. D. Dorfman, and B. Mehlig, Phys. Rev. E **92**, 062601 (2015).

[38] A. Muralidhar and K. D. Dorfman, Macromolecules **49**, 1120 (2016).

[39] A. Muralidhar, M. J. Quevillon, and K. D. Dorfman, Polymers **8**, 79 (2016).

[40] J. M. Polson, A. F. Tremblett, and Z. R. N. McLure, Macromolecules **50**, 9515 (2017).

[41] E. Werner, G. K. Cheong, D. Gupta, K. D. Dorfman, and B. Mehlig, Phys. Rev. Lett. **119**, 268102 (2017).

[42] O. Kratky and G. Porod, Recl. des Trav. Chim. des Pays-Bas **68**, 1106 (1949).

[43] N. Saitô, K. Takahashi, and Y. Yunoki, J. Phys. Soc. Jpn. **22**, 219 (1967).

[44] P. G. de Gennes, *Scaling Concepts in Polymer Physics* (Cornell University Press, Ithaca, 1979).

[45] T. Odijk, Macromolecules **16**, 1340 (1983).

[46] L. Dai, C. B. Renner, and P. S. Doyle, Adv. Colloid Interface Sci. **232**, 80 (2016).

[47] L. Onsager, Ann. N.Y. Acad. Sci. **51**, 627 (1949).

[48] J. Z. Y. Chen, Prog. Polym. Sci. **54–55**, 3 (2016).

[49] A. Khokhlov and A. Semenov, J. Stat. Phys. **38**, 161 (1985).

[50] See Supplemental Material at http://link.aps.org/supplemental/10.1103/PhysRevLett.121.037801, which includes Ref. [51], for supplemental data and figures.

[51] K. F. Freed, Adv. Chem. Phys. **22**, 1 (1972).

[52] S. M. Stavis, J. Geist, M. Gaitan, L. E. Locascio, and E. A. Strychalski, Lab Chip **12**, 1174 (2012).

[53] J. S. Leith, A. Kamanzi, D. Sean, D. Berard, A. C. Guthrie, C. M. J. McFaul, G. W. Slater, H. W. de Haan, and S. R. Leslie, Macromolecules **49**, 9266 (2016).